

# *In situ* resistance measurement of the *p*-type contact in InP–InGaAsP coolerless ridge waveguide lasers

S. B. Kuntze<sup>a)</sup> and E. H. Sargent

The Edward S. Rogers Sr. Department of Electrical and Computer Engineering  
at the University of Toronto, 10 King's College Road, Toronto, Ontario M5S 3G4, Canada

J. K. White and K. Hinzer

Bookham Inc., 1-10 Brewer Hunt Way, Kanata, Ontario K2K 2B5, Canada

St. J. Dixon-Warren

Chipworks Inc., 3685 Richmond Road, Suite 500, Ottawa, Ontario K2H 5B7, Canada

D. Ban

Institute for Microstructural Sciences at the National Research Council of Canada, 1200 Montreal Road,  
Ottawa, Ontario K1A 0R6, Canada

(Received 28 July 2004; accepted 5 January 2005; published online 18 February 2005)

Scanning voltage microscopy (SVM) is employed to measure the voltage division—and resulting contact resistance and power loss—at the *p*-In<sub>0.53</sub>Ga<sub>0.47</sub>As–*p*-InP heterojunction in a working InP–InGaAsP laser diode. This heterojunction is observed to dissipate ~35% of the total power applied to the laser over the operating bias range. This *in situ* experimental study of the parasitic voltage division (and resulting power loss and series contact resistance) highlights the need for a good *p*-type contact strategy. SVM technique provides a direct, fast and *in situ* measurement of specific contact resistance, an important device parameter. © 2005 American Institute of Physics.

[DOI: 10.1063/1.1869541]

To reduce unit cost and improve reliability, semiconductor lasers employed in short fiber optic communication links are implemented without thermoelectric coolers. A cooler adds to the overall cost and complexity of the laser package and often employs costly feedback circuitry.

Thermal management in laser design becomes critical: nonradiative carrier recombination may prevail if carriers bypass the active region by way of their thermal energy. Heating also causes threshold current to increase because more carriers on average will be able to surmount the energy barrier presented at the far side of the active region, leading to thermionic carrier leakage and lowering internal efficiency. It will be seen that a significant source of self-heating in InP–InGaAsP lasers is the *p*-type InP–InGaAs electrical contact.

In order to be considered ohmic, a contact must have a linear current-voltage characteristic resulting from good energy band alignment from one material to the next.<sup>1</sup> Ideally, the specific contact resistance  $R_c = V/J$  should be  $10^{-6} \Omega \cdot \text{cm}^2$  or less. Metal–*p*-InP contacts are predominantly nonohmic because the energy barrier from the metallic work function to the InP Fermi level is ~0.8 eV,<sup>2</sup> leading to diode (Schottky) current-voltage behavior. In particular, holes face a significant energy barrier from metal to *p*-InP and their scattering causes Joule heating of the device.

Minimizing both the specific contact resistance and the nonohmic tendencies of the contact improves device efficiency and frequency response while lowering the operating temperature.<sup>3</sup> Much research during the last two decades<sup>3–5</sup> has focused on bridging metal and *p*-InP ohmically, employing combinations and alloys of Au, Zn, Ni, Pd, Pt, Mn, Sb, W, and Ti to achieve reasonably linear *I*–*V* characteristics with  $R_c \sim 10^{-5} \Omega \cdot \text{cm}^2$ .<sup>2,6</sup>

Beyond the metallurgy of the metal–semiconductor junction, a buffer layer of highly doped InP-lattice-matched In<sub>0.53</sub>Ga<sub>0.47</sub>As reduces the compound contact resistance.<sup>7,8</sup> However, the use of a *p*-InGaAs contact layer does not entirely resolve the contact resistance problem: the layer shifts the problem from the metal–semiconductor junction to the semiconductor–semiconductor junction between the *p*-InGaAs and *p*-InP. Holes must still surmount an energy barrier ~0.45 eV between the *p*-doped binary and ternary materials.<sup>7</sup>

Conventionally, contact resistance is estimated by simulation or by isolating the contact under study in a test structure,<sup>2,7,8</sup> an example of which is shown in Fig. 1 for metal–*p*-InP via *p*-InGaAs. In the first instance, current is passed from one electrode to the other via the *p*-InGaAs layer, yielding the resistance of the metal–*p*-InGaAs contact. The InGaAs layer is then etched between the electrodes and the resistance is measured for the combined contact from

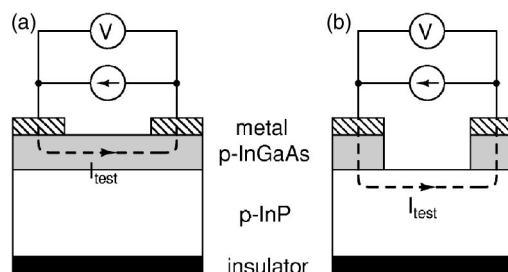


FIG. 1. Conventional method of measuring specific contact resistance of *p*-InP contact (not employed in this letter). (a) Measurement of the metal–*p*-InGaAs contact resistance. (b) The InGaAs between the electrodes is removed by etching, allowing the combined contact resistance to *p*-InP to be measured. In either case, the contact resistance for a single forward-biased metal–*p*-InGaAs–*p*-InP cannot be isolated from the combined system and must be inferred.

<sup>a)</sup>Electronic mail: scott.kuntze@utoronto.ca

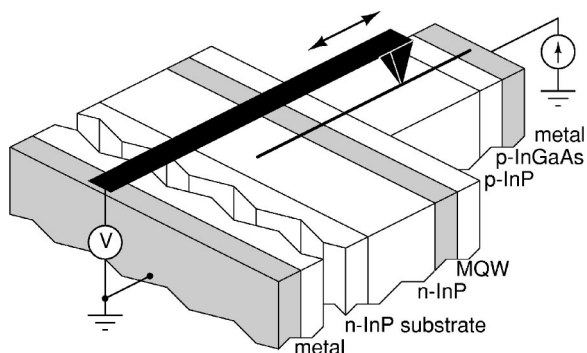


FIG. 2. Voltage scanning a ridge waveguide laser. The conductive SVM probe tip is rastered over the cleaved facet and the voltage recorded at each position.

metal to *p*-InP. There is a severe limitation of this technique: the resistance measured is influenced by both the forward and reverse contact heterojunctions of the structure. Additionally, minority electrons from vertical current leakage may influence the total resistivity in a real diode laser.<sup>9</sup> Hence, conventional methods do not directly measure the resistance of a single heterojunction in a real operating device.

In this letter, we employ scanning voltage microscopy (SVM) to image *in situ* the voltage division—and resulting contact resistance and power loss—at the *p*-In<sub>0.53</sub>Ga<sub>0.47</sub>As–*p*-InP heterojunction in a working, cooler-less laser.

Scanning voltage microscopy<sup>10,11</sup> places a nanoscopic voltage probe on an actively biased sample as illustrated in Fig. 2. A high-impedance voltmeter (input impedance  $\sim 2 \times 10^{14} \Omega$ ) ensures that negligible current is drawn from the sample and normal device operation is maintained. The voltmeter is simply used as a high-impedance buffer and its analog voltage output passed directly to data collection hardware and software. By scanning the probe over the sample surface, voltage profiles are collected.

InP–InGaAsP ridge waveguide (RWG) laser diodes were studied that emitted in the 1310 nm range and had 12 quantum wells each.<sup>12</sup> Threshold current was around 20 mA with a wallplug efficiency exceeding 0.24 mW/mA. Nominal doping concentration was  $\sim 10^{18} \text{ cm}^{-3}$  throughout the bulk InP regions; the *p*-InGaAs contact layer was doped to  $\sim 10^{19} \text{ cm}^{-3}$ . The laser cavity was cleaved at each end giving a total cavity length of 300  $\mu\text{m}$  and exposing the light-emitting facets; a schematic of a light-emitting facet is shown in Fig. 2 (the ridge is  $\sim 2 \mu\text{m}$  wide). Each laser chip was mounted on a separate heat-sinking carrier and wire-bonded to gold contacts electrically accessible to the sample holder.

3  $\mu\text{m}$  line scans with 512 samples per line were taken from the *n*-type substrate to the *p*-type metal, shown in Fig. 3. The tip velocity was 0.3  $\mu\text{m/s}$  giving 15 nm resolution on *n*-type material and 150 nm resolution on *p*-type material, limited by scan speed according to the transient analysis of Ref. 13.

SVM traces were captured over the bias range 10–190 mA in increments of 10 mA (constant current). From left to right across the position axis in Fig. 3, we observe the *n*-InP layer (the 120  $\mu\text{m}$ -thick *n*-InP substrate is not shown), multi-quantum well (MQW) active region with expected potential drop, *p*-InP ridge, large voltage drop at the *p*-InP–*p*-InGaAs interface, and transition from *p*-InGaAs to the metal contact,

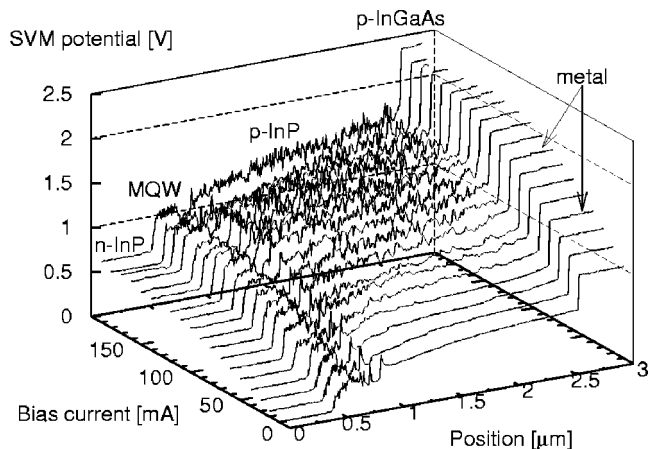


FIG. 3. SVM scans of wide-MQW RWG laser, 0:10:190 mA. The layer structure is indicated. Shot noise fluctuations increase on *p*-type material due to the wide depletion region at the tip–sample interface at high bias.

visible only as a small bump in the maximum voltage plateau (the metal and *p*-InGaAs are essentially at the same voltage). At all bias points, the voltage measured at the metal on the *p*-type side by the SVM probe is identical to the voltage measured across the terminals during a separate *V*–*I* characterization.

Dominating each SVM profile is the voltage drop across the *p*-type In<sub>0.53</sub>Ga<sub>0.47</sub>As–InP heterojunction interface. Alignment of the Fermi levels at the interface produces a valence band tunnel junction  $\sim 0.45 \text{ eV}$  tall; thermionic emission is expected to dominate<sup>7</sup> over tunneling since the barrier is relatively wide. As holes scatter at this barrier, they contribute phonons to the lattice, thereby heating the ridge and surrounding regions. The voltage drop measured by the SVM circuit reveals the change of the hole quasi-Fermi level under forward bias as described in Ref. 10.

Dividing this voltage drop  $V_{\text{het}}$  by the total voltage drop across the device,  $V_{\text{tot}}$ , yields the fractional voltage drop, power loss and series resistance at the heterojunction,

$$\frac{V_{\text{het}}}{V_{\text{tot}}} = \frac{P_{\text{het}}}{P_{\text{tot}}} = \frac{R_{\text{het}}}{R_{\text{tot}}}, \quad (1)$$

plotted in Fig. 4; the solid line is a theoretical fit of the

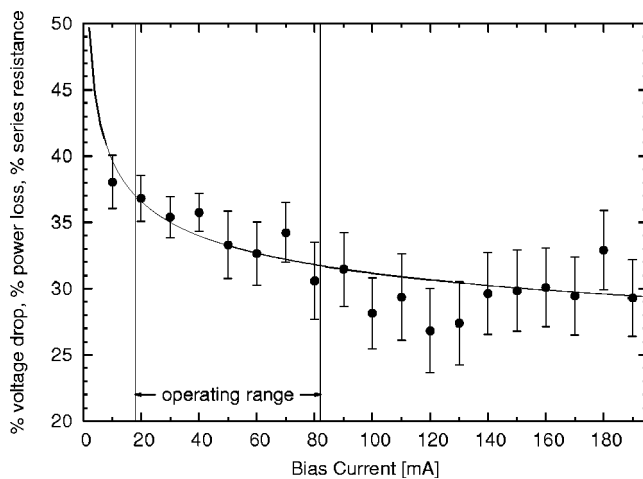


FIG. 4. Fractional parasitic voltage drop (power loss, series resistance) of *p*-InP–*p*-In<sub>0.53</sub>Ga<sub>0.47</sub>As heterojunction. The average value is 35% over the operating range. The solid line is a theoretical fit of the heterojunction voltage over the total diode voltage (see text).

heterojunction voltage over the total diode voltage,  $I_{0,\text{het}} \exp(eV_{\text{het}}/k_B T) / [I_{0,\text{tot}} \exp(eV_{\text{tot}}/nk_B T) - 1]$ . Primary uncertainty in the data arises from estimating the actual voltage of the  $p$ -type InP which is subject to shot noise fluctuations.<sup>14</sup>

It is striking that over the normal operating range of this laser (20–80 mA), approximately 35% of the wallplug power is lost before it ever reaches the active region. From the SVM profiles the  $p$ -In<sub>0.53</sub>Ga<sub>0.47</sub>As layer yields a flat, relatively lossless contact with the metal. However, a highly nonohmic contact is formed subsequently with the  $p$ -InP ridge, degrading performance and wallplug efficiency. Over the operating range the series resistance is approximately 10  $\Omega$  (estimated by dividing the heterojunction drop of Fig. 3 by the bias current<sup>15</sup>), the ridge width is  $2 \times 10^{-4}$  cm, and the cavity length is  $3 \times 10^{-2}$  cm, so the resistivity of the heterojunction is given by

$$(10 \Omega)(2 \mu\text{m})(300 \mu\text{m}) = 6 \times 10^{-5} \Omega \cdot \text{cm}^2, \quad (2)$$

nearly two orders of magnitude greater than at the metal- $p$ -InGaAs contact also measured by this SVM method.

The dissipation at the junction internally heats the laser. Heating of the active region causes carrier loss due to thermionic over-barrier leakage<sup>16</sup> which dominates the threshold current at high temperatures (80 °C) and limits the maximum lasing temperature<sup>9</sup> in ridge waveguide Fabry-Pérot architectures. Carriers possess enough energy to bypass the active region and recombine in the cladding regions either nonradiative, or radiatively at an undesired wavelength given by the bandgap of the cladding region. Thermal runaway occurs<sup>12</sup> where the increased temperature raises the threshold current and lowers the differential quantum efficiency;<sup>16</sup> pumping the laser at a higher current to maintain threshold further heats the active region, completing a thermal positive feedback loop. Ideally, forming a truly ohmic contact to the  $p$ -InP would alleviate much of the power loss and self-heating.

A method to reduce the hole barrier is to grade the  $p$ -InGaAs- $p$ -InP junction by MBE: Grading smoothes out the hole tunnel barrier and improves the specific contact resistance by an order of magnitude.<sup>7</sup> However, grading is not commonly used in practice yet these results demonstrate that an avoidable 35% of heating results from the binary-ternary contact.

SVM was applied to study the  $p$ -type contact strategy of a state-of-the-art uncooled ridge waveguide laser. Although the metal- $p$ -InGaAs contact was found to be ohmic and es-

entially lossless, the  $p$ -InGaAs- $p$ -InP heterojunction was observed to dissipate  $\sim 35\%$  of the total power applied to the laser over the operating bias range, causing self-heating. Equivalently,  $\sim 35\%$  of the series resistance is due to this heterojunction, increasing the device  $RC$  time constant and limiting frequency response. This direct study of the parasitic voltage division—and resulting power loss and series contact resistance—illustrates the need for a good  $p$ -type contact strategy.

The authors would like to thank Dr. Shiguo Zhang for helpful discussions.

<sup>1</sup>D. A. Neamen, *Semiconductor Physics and Devices: Basic Principles* (McGraw-Hill, Inc., New York, 2003), 3rd ed.

<sup>2</sup>P. W. Leech and G. K. Reeves, *Thin Solid Films* **298**, 9 (1997).

<sup>3</sup>R. Dutta, M. A. Shahid, and P. J. Sakach, *J. Appl. Phys.* **69**, 3968 (1991).

<sup>4</sup>G. Stareev, H. Künzel, and G. Dortmann, *J. Appl. Phys.* **74**, 7344 (1993).

<sup>5</sup>M.-H. Park, L. C. Wang, J. Y. Cheng, and C. J. Palmstrom, *Appl. Phys. Lett.* **70**, 99 (1997).

<sup>6</sup>A. G. Baca, F. Ren, J. C. Zolper, R. D. Briggs, and S. J. Pearton, *Thin Solid Films* **308-309**, 599 (1997).

<sup>7</sup>J. G. Wasserbauer, J. E. Bowers, M. J. Hafich, P. Silvestre, L. M. Woods, and G. Y. Robinson, *Electron. Lett.* **28**, 1568 (1992).

<sup>8</sup>P. W. Leech, G. K. Reeves, and M. H. Kibel, *J. Appl. Phys.* **76**, 4713 (1994).

<sup>9</sup>J. Piprek, P. Abraham, and J. E. Bowers, *IEEE J. Quantum Electron.* **36**, 366 (2000).

<sup>10</sup>D. Ban, E. H. Sargent, St. J. Dixon-Warren, I. Calder, A. J. SpringThorpe, R. Dworschak, G. Este, and J. K. White, *Appl. Phys. Lett.* **81**, 5057 (2002).

<sup>11</sup>D. Ban, E. H. Sargent, St. J. Dixon-Warren, I. Calder, T. Grevatt, G. Knight, and J. K. White, *J. Vac. Sci. Technol. B* **20**, 2401 (2002).

<sup>12</sup>R. Huang, J. G. Simmons, P. E. Jessop, and J. Evans, *IEEE Photonics Technol. Lett.* **9**, 889 (1997).

<sup>13</sup>S. B. Kuntze, E. H. Sargent, St. J. Dixon-Warren, J. K. White, K. Hinzer, and D. Ban, *Appl. Phys. Lett.* **84**, 601 (2004).

<sup>14</sup>The depletion region at the tip-semiconductor interface widens at higher bias (Ref. 13) and is wider for  $p$ -InP than  $n$ -InP (Refs. 13 and 17); hence, shot noise in the voltage signal is far more pronounced on  $p$ -InP due to the wide interfacial depletion region.

<sup>15</sup>To ensure that resistance is the correct interpretation, the incremental resistance of total device current-voltage characteristic and the total bulk resistance derived from SVM measurements were compared and found to agree (Ref. 18).

<sup>16</sup>L. A. Coldren and S. W. Corzine, *Diode Lasers and Photonic Integrated Circuits* (Wiley, New York, 1995).

<sup>17</sup>R. P. Lu, K. L. Kavanagh, S. Dixon-Warren, A. J. SpringThorpe, R. Streater, and I. Calder, *J. Vac. Sci. Technol. B* **20**, 1682 (2002).

<sup>18</sup>D. Ban, E. H. Sargent, St. J. Dixon-Warren, K. Hinzer, A. J. SpringThorpe, R. Streater, G. Knight, and J. K. White, *IEEE J. Quantum Electron.* **40**, 651 (2004).